A Human Neural Crest Stem Cell-Derived Dopaminergic Neuronal Model Recapitulates Biochemical Abnormalities in *GBA1* Mutation Carriers

Shi-Yu Yang,[1] Michelle Beavan,[1] Kai-Yin Chau,[1] Jan-Willem Taanman,[1] and Anthony H.V. Schapira[1,*]

[1]Department of Clinical Neurosciences, UCL Institute of Neurology, Rowland Hill Street, London NW3 2PF, UK
*Correspondence: a.schapira@ucl.ac.uk
http://dx.doi.org/10.1016/j.stemcr.2017.01.011

SUMMARY

Numerically the most important risk factor for the development of Parkinson's disease (PD) is the presence of mutations in the glucocerebrosidase *GBA1* gene. In vitro and in vivo studies show that *GBA1* mutations reduce glucocerebrosidase (GCase) activity and are associated with increased α-synuclein levels, reflecting similar changes seen in idiopathic PD brain. We have developed a neural crest stem cell-derived dopaminergic neuronal model that recapitulates biochemical abnormalities in *GBA1* mutation-associated PD. Cells showed reduced GCase protein and activity, impaired macroautophagy, and increased α-synuclein levels. Advantages of this approach include easy access to stem cells, no requirement to reprogram, and retention of the intact host genome. Treatment with a GCase chaperone increased GCase protein levels and activity, rescued the autophagic defects, and decreased α-synuclein levels. These results provide the basis for further investigation of GCase chaperones or similar drugs to slow the progression of PD.

INTRODUCTION

Parkinson's disease (PD) is a progressive neurodegenerative disorder currently affecting 4% of the population >80 years and whose prevalence is expected to double by 2030 (de Lau and Breteler, 2006). Multiple neurotransmitter systems are involved in the neurodegeneration of PD, but the loss of substantia nigra dopaminergic neurons is responsible for the dominant early motor features. The pathological hallmark of PD is the accumulation and aggregation of α-synuclein and the deposition of Lewy bodies. A heterogeneous range of etiologically and pathogenically relevant factors have been identified for PD, and it is likely that the neurodegeneration and clinical manifestations of the disease are the end result of multiple aberrant pathways (Schapira and Jenner, 2011). Several single gene defects have been identified in familial and apparently sporadic PD (Volta et al., 2015). Numerically the most important genetic risk factor for PD is the presence of mutations of the glucocerebrosidase gene *GBA1* (Sidransky et al., 2009). Although precise estimates vary between populations, approximately 5%–10% of PD patients carry *GBA1* mutations, their presence increasing the risk for PD in any one individual by 20–30 times (Beavan and Schapira, 2013).

Homozygous *GBA1* mutations are the cause of the autosomal recessive lysosomal storage disorder Gaucher disease (GD). Both homozygous and heterozygous *GBA1* mutation carriers have a similar risk for the development of PD in later life, although onset in GD patients may be earlier (Alcalay et al., 2014). The PD expressed in *GBA1*-positive patients is clinically indistinguishable from sporadic PD, except for slightly earlier onset and more cognitive dysfunction. Pharmacological responses are identical, imaging and pathology being the same as for sporadic PD (Schapira, 2015).

Interest has focused on the molecular mechanisms by which *GBA1* mutations and reduced activity of the glucocerebrosidase enzyme (GCase) increase the risk for PD. A reciprocal relationship between GCase activity and α-synuclein levels has emerged as an important candidate that may influence the development and progression of PD pathology (Sardi et al., 2015). There are several potential processes by which reduced GCase activity may result in increased α-synuclein levels and vice versa, including GCase trafficking defects, lysosomal dysfunction, substrate accumulation, and disordered lipid membrane function (Siebert et al., 2014).

To investigate further biochemical effects of *GBA1* mutations, we have developed dopaminergic neuronal lines from neural crest stem cells (NCSCs) obtained from PD and *GBA1* mutation subjects. This model has also been used to examine the potential to manipulate the GCase/α-synuclein interaction to provide candidate molecules for further investigation as disease-modifying therapies in PD. We demonstrate that these patient-derived dopaminergic cells recapitulate the main biochemical abnormalities seen in PD postmortem brain and that through the use of a small-molecule chaperone, GCase activity can be increased and α-synuclein levels reduced.

RESULTS

Isolation and Characterization of Human Adipose Neural Crest Stem Cells

Anti-aP2 antibody immunostaining was used to localize stem cell niches in blood vessel walls of human adipose tissues (Figure 1A), a feature consistent with previous observations (Shan et al., 2013). Anti-p75 neurotrophin receptor
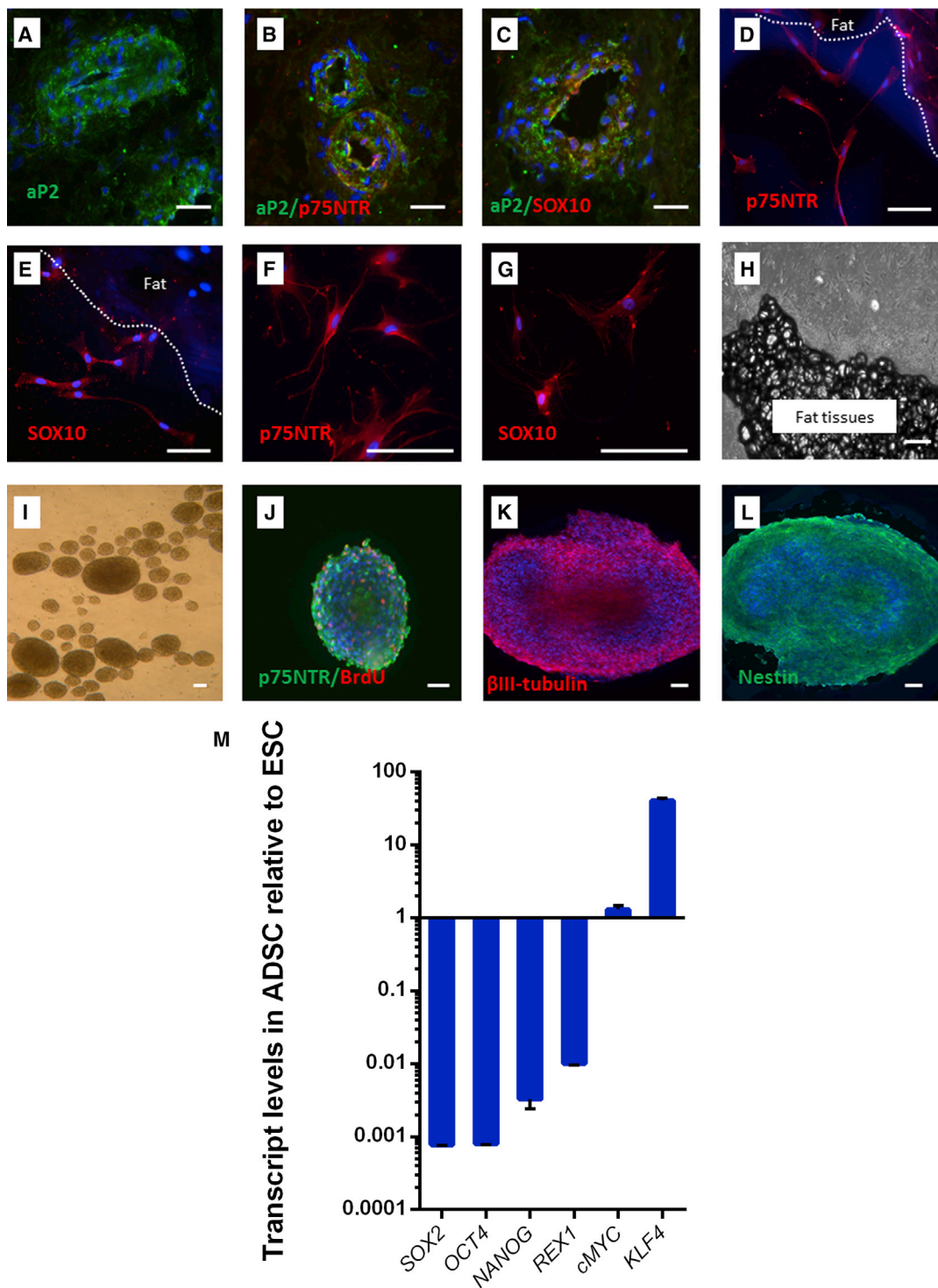
CrossMark

Figure 1. Identification, Isolation, and Characterization of Neural Crest Stem Cells from Human Adipose Tissues

(A) An anti-adipose protein 2 (aP2) antibody (green) was used to identify stem cell niches in human fat tissue.

(B and C) Two antibodies (anti-p75NTR and SOX10, both red) were employed for co-immunostaining with the anti-aP2 antibody in human adipose tissues, which revealed that some cells express p75NTR and SOX10 in the human adipose stem cell niche.

(D and E) Three to five days after explanting, human adipose tissue showed p75NTR- and SOX10-expressing cells (both red) migrating from the tissue.

(legend continued on next page)

(p75NTR) and anti-SOX10 (SOX10) antibodies were used to confirm that adipose stem cell niches contained NCSCs (Figures 1B and 1C). p75NTR is a nerve growth factor receptor highly expressed in NCSCs, and has been used to isolate NCSCs from neural tube in embryonic day 10 (E10) and E9 mice (Stemple and Anderson, 1992); SOX10 is a member of a transcription factor family (SRY-related HMG box) involved in the determination of NCSC fate and is highly expressed in NCSCs (Kim et al., 2003).

We explanted fresh human fat biopsy samples onto a 6-well plate pre-coated with fibronectin and provided energy-rich medium to enhance stem cell migration. After 3–5 days of explantation, the stem cells continuing to express p75NTR and SOX10 migrated from fat tissue (Figures 1D and 1E). After 3–4 weeks of explantation (Figure 1H), the migrated stem cells were detached using enzymatic methods, passaged, and cryopreserved. Human adipose NCSCs (haNCSCs), unlike their animal counterparts, are able to regenerate ex vivo under feeder-free conditions (Thomas et al., 2008). We cultured and maintained the stem cells under feeder-free conditions for more than 18 months with over 24 cell passages and confirmed continuing p75NTR and SOX10 expression (Figures 1F and 1G).

The ability to form neurospheres has been used to test ontogeny and multipotency of NCSCs (Nagoshi et al., 2008). haNCSCs from a range of passages were cultured in a serum-free sphere-forming medium supplemented with human epidermal growth factor, human fibroblast growth factor 2, and B27 supplement. Cells were maintained in the same medium for a further 6 days. Multiple neurospheres were formed (Figure 1I) and expressed the cell proliferation marker 5-bromo-2′-deoxyuridine (BrdU), neural progenitor maker nestin, immature neuron marker β-III tubulin, and neural crest cell marker p75NTR (Figures 1J–1L).

The pluripotent gene expression profile is varied depending on which stage the haNCSCs were isolated. If haNCSCs are isolated from the pre-migratory state in embryos, the gene expression profile is highly similar to that of human embryonic stem cells (ESCs) (Thomas et al., 2008). When haNCSCs are isolated from adult human neural crest-derived tissues, the expression of pluripotent stem genes are substantially different to human ESCs (Hauser et al., 2012). We used real-time qRT-PCR to examine the expression of six main pluripotent genes, OCT4, SOX2, NANOG, REX, cMyc, and KLF4, in haNCSCs; and compared their expression with those in a human ESC line (SHEF-6). We found that OCT4, SOX2, NANOG, and REX1 are expressed at lower levels in haNCSCs compared with that in human ESCs, in agreement with previous studies (Hauser et al., 2012), while cMyc was expressed at the same level of human ESCs and KLF4 was expressed at a higher level compared with human ESCs (Figure 1M). KLF4 is a transcriptional regulator of genes critical for epithelial-mesenchymal transition (Tiwari et al., 2013), which is pre-step of neural crest cells migrating to various elected locations during embryo development (Nagoshi et al., 2008). As we used the migration procedure to isolate haNCSCs, the higher level of KLF4 in haNCSCs than ESCs is to be expected.

A recent study comparing regulatory programs between neural crest cells and early ESCs found that neural crest cells retain core pluripotency genes (Buitrago-Delgado et al., 2015). We therefore examined the expression of the pluripotent genes NANOG, OCT4, SSEA4, and TRA-1-81, and the neural crest genes p75NTR and SOX10. HaNCSCs were isolated from age-matched controls, individuals with heterozygous GBA1 (N370S/WT) mutations, and sporadic PD patients (for details see Table S1). The results showed that pluripotent and neural crest genes were expressed in all haNCSC lines, indicating that they retain neural crest cell features and pluripotent properties (Figures S1A–S1C). There were no differences in the expression of these genes between the haNCSC lines. Sonic hedgehog (SHH) is a signaling molecule that has been found to be involved in the development of early neural crest progenitors (Brito et al., 2006; Wada et al., 2005) and promotes the formation of multipotent progenitors endowed with both neural-melanocytic and mesenchymal differentiation potential (Calloni et al., 2007; Le Douarin et al., 2004). SHH executes its functions through a cell-surface transmembrane protein called Patched (PTCH) and a membrane-spanning receptor called Smoothened (SMO). We therefore examined the expression of PTCH and SMO in three groups

(F and G) Migrated cells were cultured and maintained under feeder-free conditions for more than 18 months with more than 24 cell passages and still expressed p75NTR and SOX10 (both red).
(H) Three-week-old human adipose explant showing numerous cells that migrated from the tissue.
(I) Neurospheres formed after 6 days of culturing in neurosphere formation medium.
(J) The cell proliferation marker BrdU (red).
(K and L) The neuronal marker β-III tubulin (red) and the neuronal progenitor maker nestin (green) were expressed in the neurospheres. Nuclei were stained with DAPI (blue).
(M) The pluripotent gene expression in haNCSC was examined by real-time qRT-PCR and compared with human ESC line (SHEF-6). ADSC, adipose-derived stem cells. Relative expression values are plotted as means ± SEM from three independent experiments (n = 3).
Scale bars, 50 μm.

of haNCSCs with flow cytometry analysis. More than 60% of cells stained positive with both PTCH and SMO proteins (Figure 1D), and there were no significant differences in the levels of these proteins between three haNCSC groups. These data support the conclusion that adult human adipose tissue contains a cell population that retains neural crest cell features and can be isolated with a simple migration protocol.

Dopaminergic Neuronal Differentiation of haNCSCs

A mouse stromal cell (PA6) line has been shown to be able to induce ESCs to form midbrain dopaminergic neurons (Kawasaki et al., 2000). We therefore initially used PA6 cells for haNCSC dopaminergic neuronal differentiation via a co-culture procedure. After co-culturing with a PA6 cell line for 40 days, haNCSCs were successfully induced to dopaminergic neurons, which express midbrain dopaminergic neuronal makers such as tyrosine hydroxylase (TH) (Figure 2A), dopamine transporter (DAT) (Figure 2A), LIM-homeobox transcription factor 1 (LMX1) (Figure 2A), nuclear receptor-related protein 1 (NURR1) (Figure 2A), and a general neuronal marker, β-III tubulin (Figure 2A). However, to generate more pure dopaminergic haNCSC cultures, we used a defined dopaminergic neuronal differentiation program proven to be able to generate midbrain dopaminergic neurons from human mesenchymal stem cells (Trzaska and Rameshwar, 2011). During the differentiation cells change their morphology toward neuron-like cells (Figure 2B), and express the neuronal marker β-III tubulin after 6 days (Figure 2C) and the dopaminergic neuronal makers TH and DAT after 12 days (Figure 2C). Following 40 days differentiation, the neurons become more mature and express both dopaminergic neuronal markers TH and midbrain neuronal markers NURR1 (Figure 2D). The proportion of dopaminergic neurons (TH$^+$) derived from control, heterozygous mutant *GBA1*, and PD subjects was not significantly different (Figures 2D and 2E). The percentage of TH$^+$ neurons was 38%–52% (Figure 2E).

To examine the maturation and function of neuronal cells, we examined the expression of functional ligand-gated channels in differentiated neurons by measuring intracellular Ca^{2+} changes upon application of the neuronal transmitters (glutamate, dopamine, and N-methyl-D-aspartate [NMDA]) in cells loaded with Fluo-4 AM or Fura-2 AM. After 40 days of neuronal differentiation, up to 56% of cells responded to dopamine and 21% responded to glutamate (Figures 2F and 2G), indicating that haNCSCs can be differentiated to functional dopaminergic neuronal cells.

Establishment of haNCSC-Derived Neuronal Models of *GBA1*-Associated PD

To investigate the effects of heterozygous *GBA1* mutations on GCase activity and protein levels in neuronal cells, we

differentiated haNCSC cell lines from wild-type (WT; control) and heterozygous *GBA1* N370S/WT mutation (Table S1) to dopaminergic neuronal cells using the program described above. The cells were harvested at different stages (0, 20, and 40 days) of the differentiation program. The GCase activity was measured with a fluorogenic assay, and GCase protein level was determined by western blotting. The results showed that both the protein level and activity of GCase increased significantly in the WT stem cell-derived neurons compared with undifferentiated stem cells during differentiation (Figures 3A–3C). These increases did not occur in *GBA1* mutant (N370S/WT) haNCSC-derived neurons (Figures 3A–3C).

Induced pluripotent stem cell (iPSC)-derived neurons from *GBA1* mutation patients show reduced GCase enzymatic activity and protein levels (Schondorf et al., 2014). To validate and compare the abnormality seen in the haNCSC-derived heterozygous *GBA1* mutant neurons, we generated iPSCs from fibroblasts from control subjects and subjects heterozygous for the N370S *GBA1* mutation (Okita et al., 2011). The iPSC clones from both control and mutant subjects expressed pluripotent genes (*NANOG*, *SSEA4*, *TRA-1-81*, and *OCT4*), and the expression of the pluripotent genes between control and *GBA1* mutation subjects was not significantly different (Figure S2A). Karyotyping results revealed that no translocations had occurred during cloning of iPSC (Figure S2C). The iPSC stem cells were differentiated into dopaminergic neurons expressing the neuronal marker (β-III tubulin) and dopaminergic neuronal markers TH and Nurr1 (Figure S2B). Although the pluripotent properties of iPSC clones were not significantly different between control subjects and subjects heterozygous for the *GBA1* mutation, the GCase activity and protein level were significantly reduced in neurons derived from subjects heterozygous for the *GBA1* mutation differentiation (Figures 3D–3F). These results are not only consistent with the previous iPSC studies, but also confirm the abnormality seen in the haNCSC-derived heterozygous *GBA1* mutant neurons (Figures 3A–3C). The level of β-III tubulin expression in the haNCSC-derived neurons is constant at 40–50 days of differentiation, suggesting that the neuronal cell population is stable at this time in both control and *GBA1* mutation subjects (Figures 3G and 3H). We therefore selected this time period to examine the effects of therapeutic intervention with ambroxol.

Heterozygous *GBA1* Mutations Decrease GCase Activity and Protein Levels in Human Neurons

A recent study using iPSCs with homozygous *GBA1* mutations described widespread lysosomal depletion (Awad et al., 2015). To investigate the effects of heterozygous *GBA1* mutations on GCase activity, we differentiated
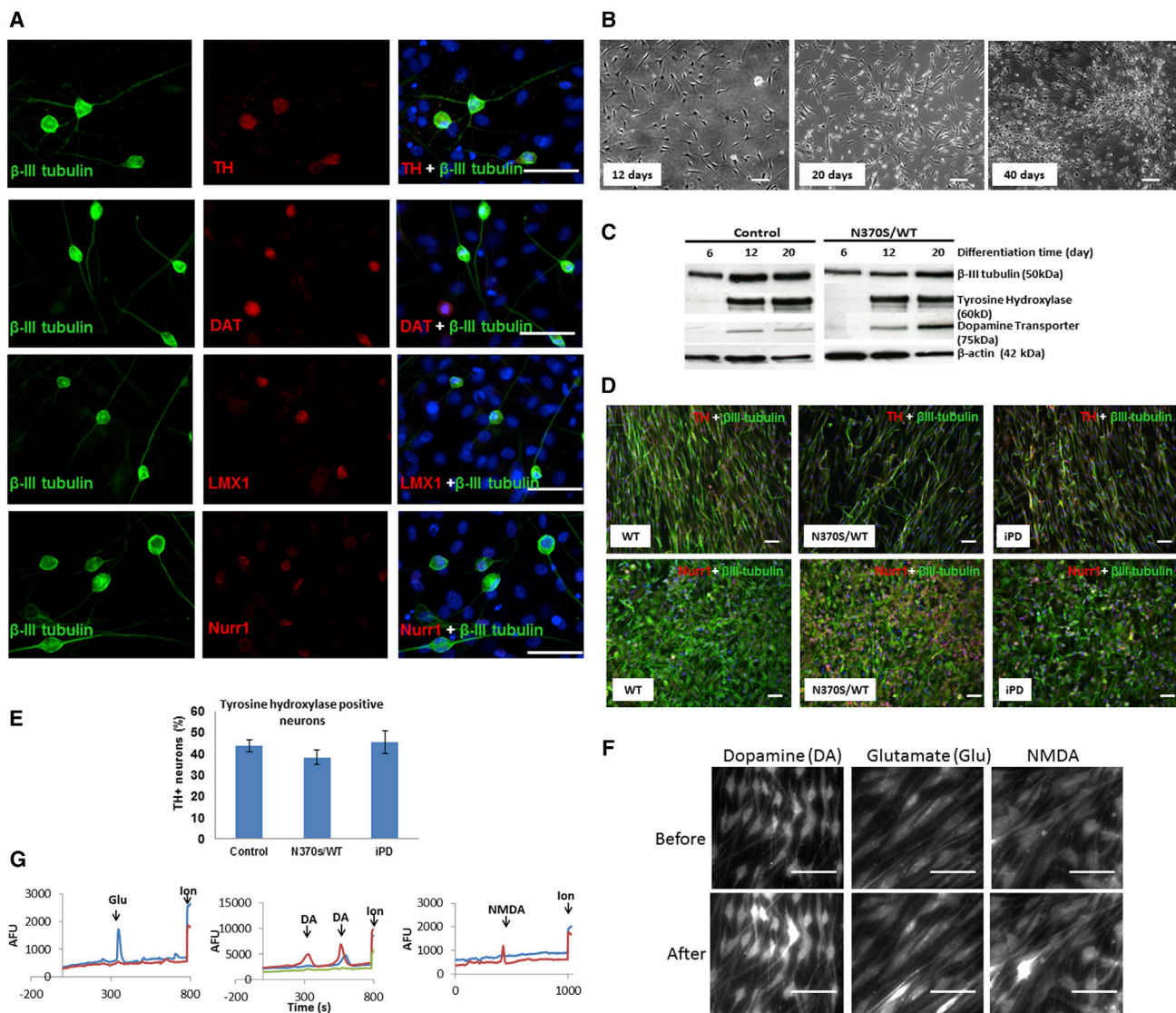
Figure 2. Dopaminergic Neuronal Differentiation of haNCSCs

(A) The mouse PA6 cell line was used for dopaminergic neuronal differentiation via a co-culture procedure. After co-culturing for 40 days, human adipose neural crest stem cells expressed the dopaminergic neuronal makers tyrosine hydroxylase (TH, red) and the dopamine transporter (DAT, red), the midbrain markers LIM-homeodomain transcription factor (LMX1, red), and nuclear receptor-related protein 1 (Nurr1, red) and the pan-neuronal marker β-III tubulin (green).

(B) When a defined program was used to differentiate adipose neural crest stem cells into dopaminergic neurons, the cells gradually changed their morphology toward neuron-like cells.

(C) Western blot experiments showed that pan-neuronal (β-III tubulin) and dopaminergic neuronal makers (TH, DAT) were expressed after 20 days of defined neuronal differentiation.

(D and E) After 40 days of defined neuronal differentiation, the percentage of TH$^+$ neurons was 38%–52%. The proportion of TH$^+$ neurons derived from wild-type (WT) control, heterozygous mutant *GBA1*, and iPD subjects was not significantly different. For all three groups n = 3 cell lines, and data are represented as mean ± SEM.

(F and G) The expression of functional ligand-gated channels in differentiated neurons was examined by measuring cytosolic Ca^{2+} changes (bright) upon application of the neural transmitters (glutamate, dopamine, and NMDA) in cells loaded with Fluo-4 AM or Fura-2 AM. After 40 days of defined neuronal differentiation, up to 56% of cells responded to dopamine (DA), 21% responded to glutamate (Glu), and 16% responded to NMDA. Nuclei were stained with DAPI (blue). AFU, arbitrary fluorescence units.
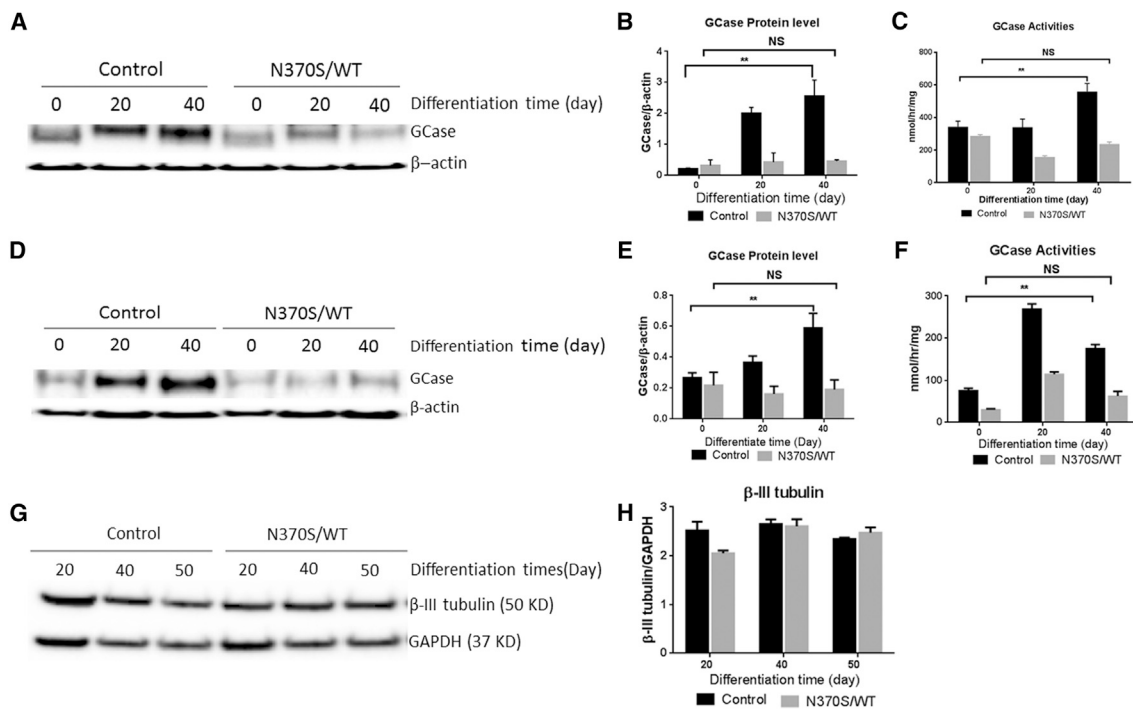
Scale bars, 50 μm.

Figure 3. Establishment of haNCSC-Derived Neuronal Models of *GBA1*-Associated PD

(A and B) Control and N370S/WT haNCSC lines were differentiated to dopaminergic neurons with the defined program. The GCase protein levels increased significantly in control haNCSC-derived neurons during differentiation, but were not increased in *GBA1* mutant (N370S/WT) haNCSC-derived neurons.

(C) The activity of GCase also increased significantly in control haNCSC-derived neurons during differentiation, but this increase was not seen in *GBA1* mutant (N370S/WT) haNCSC-derived neurons.

(D–F) Likewise, the GCase protein levels and activity in the iPSC-derived neurons increased significantly during differentiation in control subjects but not in subjects heterozygous for the *GBA1* mutation.

(G and H) By examining the neuronal marker β-III tubulin in the differentiated cells, it was found that 40–50 days of differentiation is the optimal time window to examine the effects of therapeutic interference.

Data are presented as means ± SEM from three independent experiments (n = 3). **p < 0.01; NS, not significant (p > 0.05). All comparisons were carried out with one-way ANOVA and Student's t test.

haNCSCs derived from controls and subjects heterozygous for the *GBA1* mutation (N370S/WT) and idiopathic PD (iPD) into dopaminergic neurons with the established differentiation program for 40 days. GCase activity was significantly reduced by 40.2% (p = 0.0307) in the *GBA1* mutation group compared with control. GCase activity was not reduced in the iPD-derived neurons (Figure 4A). Hexosaminidase activity, another lysosomal enzyme, was not significantly different in the different cell lines (Figure 4B). The GCase protein level in N370S/WT stem cell-derived neurons was significantly decreased by 61.3% (p = 0.0257) compared with WT (Figures 4C and 4E), consistent with previous iPSC-derived neuronal studies (Schondorf et al., 2014). There was a trend for the GCase protein level in idiopathic PD stem cell-derived neurons to be decreased, but this was not statistically significant.

GBA1 Mutation Increased α-Synuclein Level in haNCSC-Derived Dopaminergic Neurons

Inhibition of GCase led to the accumulation of α-synuclein in in vitro and in vivo models (Cleeter et al., 2013; Manning-Bog et al., 2009). The iPSC-derived neuronal model from both GD and heterozygous *GBA1* mutant demonstrated accumulation of α-synuclein (Mazzulli et al., 2011). In our model, the level of α-synuclein was significantly increased by 172% (p = 0.02) in the neurons derived from *GBA1* mutation haNCSC-derived dopaminergic neurons compared with controls (Figures 4D and 4F). Immunocytochemistry in the GBA1 mutant (N370S/WT) human neurons showed that the level of α-synuclein protein was higher in the dopaminergic as opposed to the non-dopaminergic cells in culture (Figures 4G and 4H). There was a trend for the level of α-synuclein in the idiopathic PD group to be
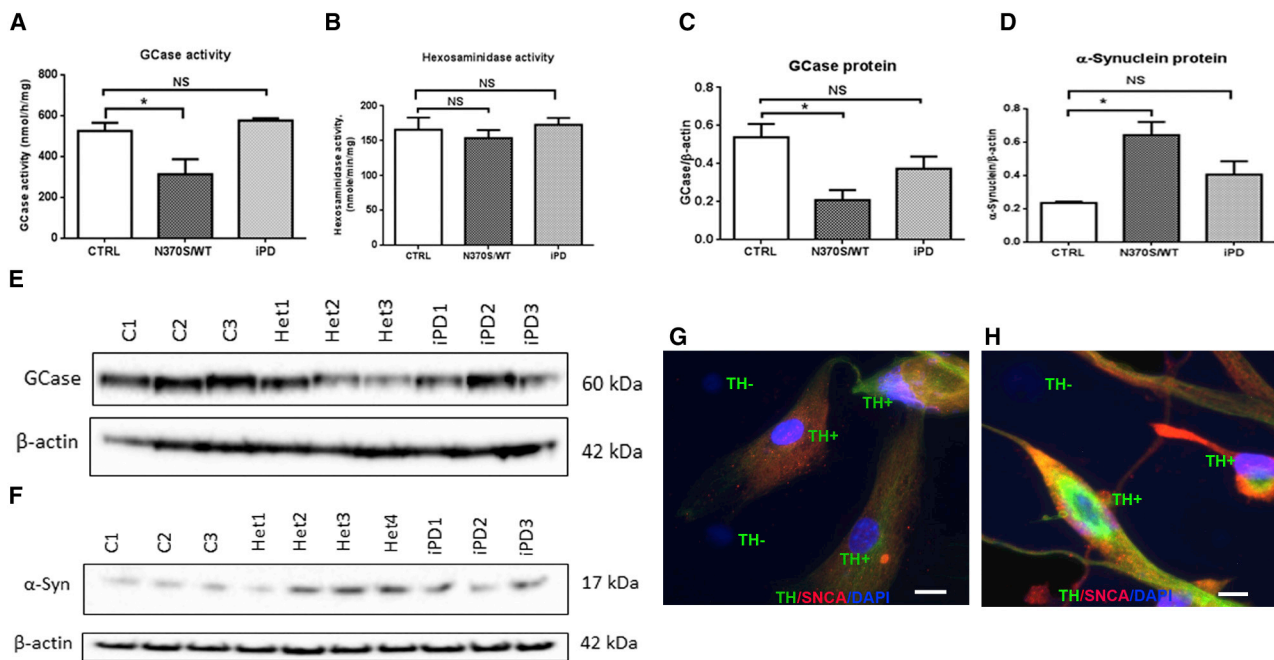
Figure 4. *GBA1* Mutation Decreases GCase Activity and Protein Levels and Increases α-Synuclein in haNCSC-Derived Dopaminergic Neurons

(A, C, and E) HaNCSCs derived from controls (CTRL, C1–3), carriers of the heterozygous *GBA1* mutation (N370S/wt; Het1–3), and idiopathic Parkinson's disease (iPD1–3) patients were differentiated into dopaminergic neurons for 40 days. GCase activity and the level of GCase protein were significantly lower in the *GBA1* mutation group, but not in the iPD group, compared with the control group. For all three groups n = 3 cell lines; data are represented as mean ± SEM.

(B) Hexosaminidase, another lysosomal enzyme, was not affected by the *GBA1* mutation. For all three groups n = 3 cell lines; data are represented as means ± SEM.

(D and F) The level of α-synuclein was significantly increased in the *GBA1* mutation group, but not in iPD group, compared with the control group. For both control and iPD groups n = 3 cell lines; for the *GBA1* mutation group (Het1–4) n = 4 cell lines; data are represented as mean ± SEM.

(G and H) The level of α-synuclein protein (red) was identified in the untreated *GBA1* mutant (N370S/WT) human neurons. Results indicate that dopaminergic neurons (TH⁺, green) have a higher level of α-synuclein protein. Nuclei were stained with DAPI (blue).

All comparisons were carried out with one-way ANOVA and Student's t test. *p < 0.05; NS, not significant (p > 0.05). Scale bars, 10 μm.

elevated, but this did not reach statistical significance (Figures 4D and 4F).

GBA1 Mutation Impaired Macroautophagy in haNCSC-Derived Dopaminergic Neurons

Postmortem PD brain (Murphy et al., 2014) and an iPSC-derived neuronal model from *GBA1* mutant PD patients (Schondorf et al., 2014) suggested that GCase deficiency may cause general autophagic dysfunction and disruption of the autophagy-lysosome pathway. We found that basal levels of light chain type 3-II protein (LC3-II), a marker of autophagosomes, were decreased, but not significantly so, in *GBA1* mutation-positive carrier neurons compared with control neurons (Figures 5A and 5B). The decrease of LC3-II in *GBA1* mutation-positive carrier neurons suggests, but does not confirm, that the N370S *GBA1* mutation impairs autophagosome formation.

P62 is a ubiquitin-binding scaffold protein acting as a cargo receptor recruited to the autophagosome membrane through interaction with LC3-II (Itakura and Mizushima, 2011), and is an alternative marker for detecting autophagic flux (Bjorkoy et al., 2005). P62 levels were decreased 62% (p = 0.0162) in *GBA1* mutant neurons (Figures 5C and 5D). To examine whether the decrease in LC3-II and p62 is due to a defect of the fusion of autophagosomes with lysosomes or to dysfunction of autophagosome formation, we inhibited the macroautophagy pathway at the autophagosome-lysosome fusion stage with bafilomycin. The results (Figures 5E–5H) showed that LC3-II and p62 protein levels were increased significantly after bafilomycin treatment. This indicates that the autophagosome-lysosome fusion pathway was normal and that the decrease in LC3-II and p62 protein levels in *GBA1* mutation neuronal cells are most likely due to impaired autophagosome formation.
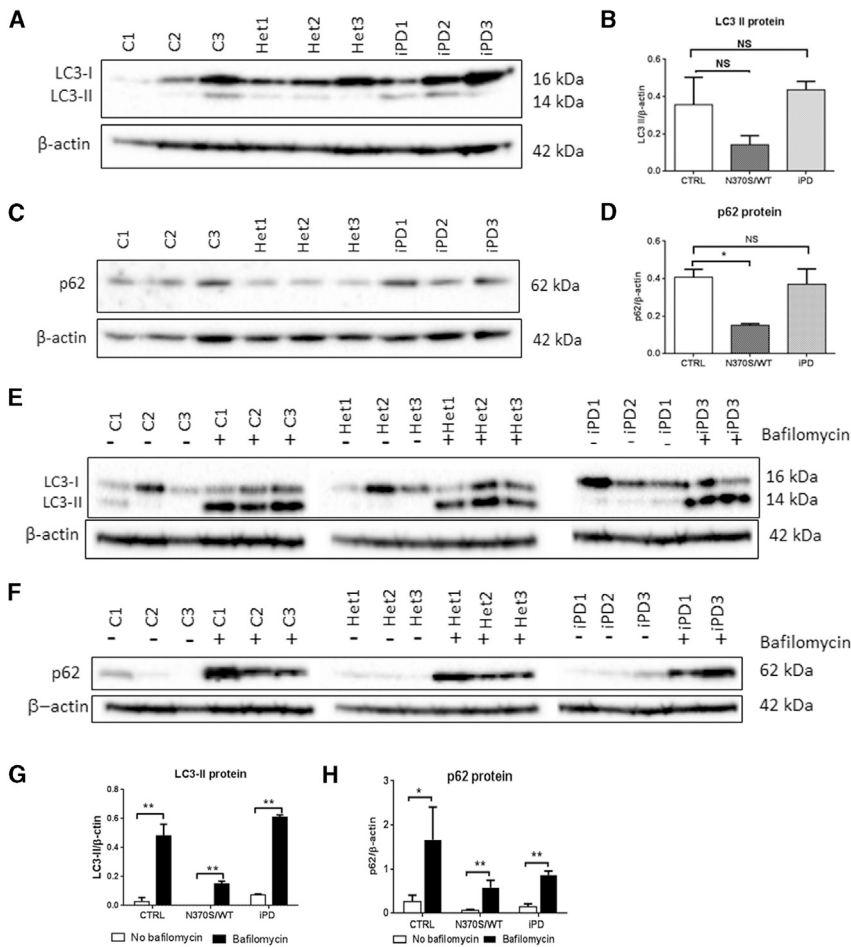
Figure 5. HaNCSC-Derived Dopaminergic Neurons from *GBA1* Mutant Carriers Show Defective Lysosomal Autophagy

(A and B) LC3-II appeared decreased in the *GBA1* mutation group (N370/wt; Het1–3) compared with the control (C1–3; CTRL) and iPD (PD1–3) groups, but the decrease was not statistically significant.

(C and D)The ubiquitin-associated protein p62 was significantly decreased in the *GBA1* mutation group compared with the other two groups.

(E–H) When the neurons were incubated with the inhibitor of autophagy bafilomycin, the LC3-II and p62 level increased significantly, indicating that the fusion of lysosomes with autophagosome was normal but the autophagosome number was reduced by the *GBA1* mutation; i.e., the creation of autophagosomes in the *GBA1* mutant neurons was decreased.

For all three groups n = 3 cell lines; data are presented as means ± SEM. All comparisons were carried out with one-way ANOVA and Student's t test. **p < 0.01; *p < 0.05; NS, not significant (p > 0.05).

GBA1 Mutation Does Not Affect LAMP2a or LAMP1

There was no significant change in levels of the chaperone-mediated autophagy (CMA) protein LAMP2a or LAMP1 in *GBA1* mutation carrier neurons when compared with control cells (Figures S3A–S3D).

Ambroxol Treatment Increases GCase Activity and Protein Levels

Ambroxol is a GCase small-molecule chaperone that has been reported to increase the expression of the *TFEB* transcription factor (McNeill et al., 2014). Ambroxol was incubated for 6 days with 40-day differentiated dopaminergic neurons derived from haNCSCs and induced a significant increase in GCase activity (CTRL 34.8% [p = 0.164], *GBA1* mutation 70.6% [p = 0.0004], and iPD 28.6% [p = 0.016]) and protein levels (CTRL 65.2% [p = 0.026], *GBA1* mutation 330.2% [p = 0.009], and iPD 190.7% [p = 0.050]) in all tested lines (Figures 6A, 6B, and 6D). Any contribution from non-lysosomal GCase (*GBA2*) was identified by using the inhibitor conduritol-B-epoxide (CBE) (Figure 6B). CBE inhibition of the haNCSC-derived neuronal cell lines led

to 90% GCase inhibition in all cell lines. There was no significant change in hexosaminidase activities after ambroxol exposure (Figure 6C).

Ambroxol Reduces α-Synuclein Levels in *GBA1* Mutant Neurons

A significant increase in α-synuclein protein levels was found in 40-day-old *GBA1* mutation-positive haNCSC-derived neurons carrying the N370S allele compared with controls (Figure 4F). Following ambroxol treatment, there was a significant reduction in α-synuclein levels in the *GBA1* mutation neurons (by 83%, p = 0.025). α-Synuclein levels were also reduced in control and iPD neurons, but these did not reach significance (35% [p = 0.316] and 39% [p = 0.267], respectively) (Figures 6E and 6F). α-Synuclein mRNA levels were not affected in any of the neuronal lines before or after ambroxol treatment (Figure 6G). Immunochemical staining of α-synuclein in untreated N370S mutant neurons (Figures 6K and 6L) and treated N370S mutant neurons (Figures 6M and 6N) indicated that ambroxol reduced α-synuclein levels in neurons.

Because it has been reported that cathepsin D is important in the degradation of α-synuclein (Sevlever et al., 2008), we investigated whether ambroxol modulated the level of this protein in the patient-derived cells. We found that the level of mature cathepsin D protein in *GBA1* mutant (N370S/WT) neurons increased following ambroxol treatment (Figures 6I and 6J).

Ambroxol Treatment Upregulates Macroautophagy and Rescues Autophagy

Following 6 days of ambroxol treatment, there was an upregulation of macroautophagy with significant increases seen in both LC3-II (Figures 7A and 7C) and p62 (Figures 7B and 7D) protein levels in *GBA1* mutation-positive and iPD neurons. Incubation of differentiated neurons with bafilomycin for 4 hr caused a further increase in LC3-II and p62 protein in all lines (Figures 7G–7J), indicating that ambroxol-increased LC3-II and p62 was not due to blockade of the autophagosome-lysosome fusion pathway. LC3B mRNA levels were not significantly increased after ambroxol treatment (Figure 7E). p62 mRNA was significantly increased in the PD group after ambroxol treatment; there was a trend toward increased *GBA1* mutant neurons, but this did not reach significance (Figure 7F). Ambroxol did not affect hexosaminidase activity (Figure 6C) or levels of LAMP1 and LAMP2a (Figures S4A–S4D).

DISCUSSION

Our study describes the preparation and analysis of dopaminergic neurons from NCSCs isolated from human adipose tissue, their use in the investigation of the biochemical consequences of the *GBA1* N370S mutation, and the potential for the small-molecule GCase chaperone, ambroxol, to reverse these effects. The use of haNCSCs provides direct access to pluripotent stem cells and provides an alternative source to those derived from fibroblast lines for the creation of neuronal lines. The haNCSC approach has advantages in terms of ease of access to neural crest cells, no requirement to reprogram, retention of the intact host genome, simple protocols for neuronal differentiation, production of homogeneous colonies, and less cost.

We have used this technique to develop both haNCSCs and iPSCs from controls and patients with the N370S *GBA1* mutation that causes GD and increases the risk for PD. Cell lineages were differentiated into dopaminergic neurons and compared with data from iPSCs derived from fibroblasts from the same donors. Compared with controls, the N370S mutant lines from both sources showed reduced GCase activity and protein levels and increased α-synuclein levels. These results are in agreement with a previous study using PD-derived iPSCs (Schondorf

et al., 2014). We also show that the small-molecule GCase chaperone ambroxol can rescue GCase activity and reduce α-synuclein levels in human neurons. A recent study (Mazzulli et al., 2016) used a non-inhibitory small modulator to activate GCase in synucleinopathy culture model and found that activation of GCase enhanced the clearance of pathological α-synuclein. These findings support the hypothesis that increasing GCase activity reduces α-synuclein levels in dopaminergic neurons, and has significant implications for the use of GCase chaperones as treatments to reduce α-synuclein in PD patients.

Our results also have several important implications for the future study of *GBA1* mutations in PD. The ability easily to generate dopaminergic neurons from stem cells derived directly from the host provides an important source for the study of the biochemical consequences of GCase deficiency. We show that the N370S mutation reduces GCase protein levels and activity, and is associated with elevated α-synuclein levels. These are the core biochemical features in the study of *GBA1* mutations in PD as expressed in PD brain (Gegg et al., 2012) and provide a model with which to test therapeutic interventions to manipulate the GCase-α-synuclein pathway.

We show that the GCase defect was associated with impaired autophagosome formation in the N370S *GBA1* mutation dopaminergic haNCSCs, in agreement with Schondorf et al. (2014). We have shown that ambroxol rescues the biochemical abnormalities resulting from the N370S mutation. Ambroxol increased GCase activity in GD and PD fibroblasts and reduced α-synuclein levels in SHSY-5Y cells (McNeill et al., 2014). Ambroxol has also been shown to activate transcription factor EB and therefore to induce transcriptional upregulation of the CLEAR (coordinated lysosomal expression and regulation) network and saposin C levels (Ambrosi et al., 2015; McNeill et al., 2014). In the dopaminergic neuronal model derived from haNCSCs, ambroxol significantly increased GCase protein in the idiopathic PD and N370S *GBA1* mutant lines. There were parallel increases in activity in the N370S and iPD lines, with a trend in the controls that did not reach significance. We also found that ambroxol can significantly increase mature cathepsin D protein in N370S *GBA1* mutant lines. This may be a consequence of the transcriptional effects of ambroxol and may contribute to the mechanisms by which this drug reduces α-synuclein levels. An alternative or additional mechanism for the reduction in α-synuclein may be an increase in cathepsin D due to elevated GCase and ceramide levels induced by ambroxol.

Autophagy is considered to be a dynamic process comprising three sequential steps: formation of autophagosomes, the fusion of autophagosomes with lysosomes, and degradation. During this process, cytosolic form of
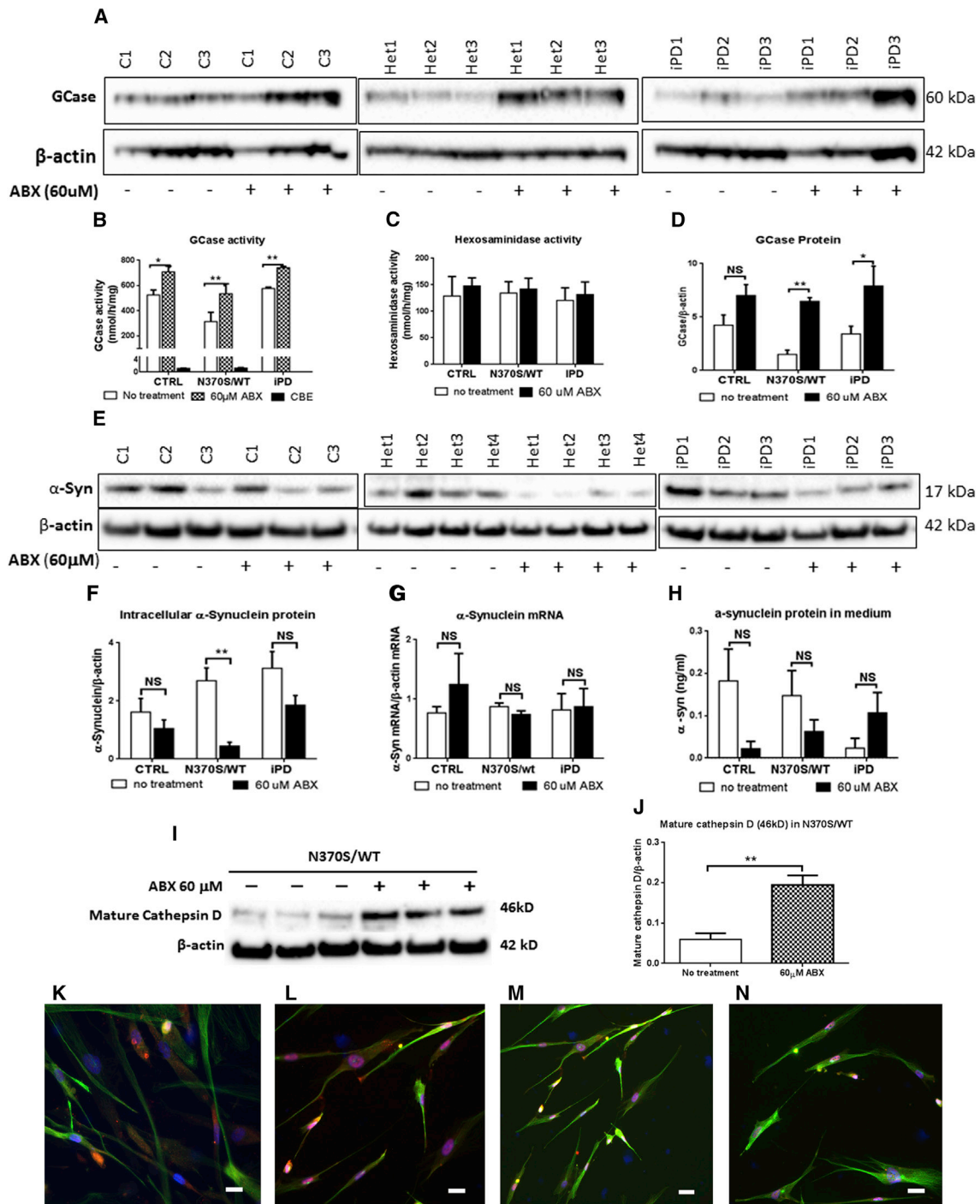
Figure 6. Ambroxol Treatment Recovers GCase Activity and Increases GCase Protein

(A and D) The level of GCase protein was increased following ambroxol (ABX) treatment in heterozygous *GBA1* mutant (Het1–3; N370S/wt) and iPD (PD1–3) neurons, but not in neurons derived from controls (C1–3; CTRL). For all three groups n = 3 cell lines.

(B) Ambroxol treatment significantly increased GCase activity in all three groups of neurons. Addition of the GCase inhibitor, conduritol-B-epoxide (CBE), showed that the contribution to the increase from non-lysosomal GCase (*GBA2*) was minimal. For all three groups n = 3 cell lines.

(C)The activity of hexosaminidase was not affected by ambroxol treatment. For all three groups n = 3 cell lines.

(legend continued on next page)

LC3 is conjugated with phosphatidylethanolamine to form LC3-II, which is recruited to autophagosome membranes. p62 is a ubiquitin-binding scaffold protein acting as a cargo receptor, which is recruited in the formation of autophagosomes (Itakura and Mizushima, 2011). Ambroxol treatment significantly increased the steady-state levels of both LC3-II and p62 proteins in our model, suggesting that ambroxol increases autophagy by promoting autophagosome formation and turnover. This interpretation is further supported by a substantial increase in p62 mRNA. The unaltered LC3B gene expression suggests that the influence of ambroxol on LC3 synthesis is minimal.

The autophagic pathway has been increasingly implicated in a number of neurodegenerative diseases including PD (Mizushima et al., 2008), and the deregulation of autophagy is evident in the brains of PD patients (Levy et al., 2009). Autophagy has three different pathways, namely macroautophagy, microautophagy, and CMA. Previous studies have found that both macroautophagy and CMA pathways contribute to α-synuclein degradation in primary postnatal ventral midbrain neurons (Xilouri et al., 2008). Directly applying bafilomycin A1, an inhibitor of autophagy, to the cortex of α-synuclein transgenic mice increased α-synuclein levels in brain (Ebrahimi-Fakhari et al., 2012), suggesting that the autophagic pathway plays an important role in degradation of α-synuclein in neurons. Ambroxol treatment restores autophagosome formation in GBA1 mutant lines, which in turn would enhance the degradation of α-synuclein and contribute to the decreased α-synuclein levels in the GBA1 mutant lines. These results are important in confirming in patient-derived dopaminergic neuronal cells that ambroxol can rescue defects due to GCase deficiency, and appears to do so by several mechanisms. The reduction in neuronal α-synuclein levels offers the potential for ambroxol or similar drugs to be tried as a disease-modifying therapy in PD patients with GBA1 mutations (Schapira and Gegg, 2013). The strategy to reduce α-synuclein in PD is common

to a number of approaches to slow progression in PD (Schapira et al., 2014). Ambroxol is currently under investigation to confirm blood-brain barrier penetration before use in a larger trial. However, the haNCSC dopaminergic model used here provides the opportunity to test similar drugs to manipulate the GCase pathway for neuroprotection in PD.

EXPERIMENTAL PROCEDURES

Subjects and Sample Collection
Samples from ten subjects were used in the study; written informed consent was obtained before subcutaneous fat was collected. The protocols used for collection were approved by the Royal Free Research Ethics Committee (REC number 10/H0720/21). PD was diagnosed according to UK Brain Bank criteria (Litvan et al., 2003). Differences in age and sex between groups were checked using one-way ANOVA. Skin-punch biopsies containing subcutaneous adipose tissues (4 mm in diameter) were obtained from arm of participants; the subcutaneous adipose tissues were dissected from skin and used for cell isolation. Ten subjects were divided into three groups according to their genotype (wt/wt healthy, N370S/wt, and wt/wt iPD). In some of the experiments we used four heterozygous mutation lines including three heterozygous carriers and one heterozygous PD. This was initially to examine whether there were differences between these cell lines in terms of changes associated with the GBA1 mutation. We examined GCase activity, SNCA, and LAMP1 protein level in all of these four cell lines before and after ambroxol treatment, and found that the changes in these four cell lines are all similar; we have not observed any significant differences between heterozygous carriers and heterozygous PD cell lines. Therefore, we used three heterozygous carriers for the remainder of the experiments. More detailed information regarding subjects can be found in Table S1.

Isolation and Maintenance of haNCSCs
Human subcutaneous adipose tissues were washed once with growth medium and dissected into small pieces (less than 0.2 cm diameter). The small pieces of adipose tissues were explanted in fibronectin-coated 6-well plates. A sterilized coverslip was used to

---

(E and F) Ambroxol treatment (60 μM) significantly decreased α-synuclein protein in *GBA1* mutant (N370S/WT) neurons. The lower level of α-synuclein protein also occurred in treated WT and iPD neurons, but the decrease was not significant. For control and iPD groups n = 3 cell lines; for the *GBA1* mutant group n = 4 cell lines.

(G) The α-synuclein mRNA level in all three groups of neurons was not affected by ambroxol treatment. For control and iPD groups n = 3 cell lines; for *GBA1* mutant group n = 4 cell lines.

(H) There was no significant difference in the amount of α-synuclein released in the culture medium between treated and untreated cells of all three groups. For control and iPD groups n = 3 cell lines; for *GBA1* mutant group n = 4 cell lines.

(I and J) Mature cathepsin D protein level was significantly increased following ambroxol treatment in *GBA1* mutant (N370S/WT) human neurons. For all groups n = 3 cell lines.

(K and L) High level of α-synuclein protein (red) was seen in untreated in the *GBA1* mutant (N370S/WT) neurons.

(M and N) The lower level of α-synuclein protein (red) was seen in the ambroxol-treated *GBA1* mutant (N370S/WT) neurons. The neuronal marker β-III tubulin was stained green. Nuclei were stained with DAPI (blue).

Data are presented as means ± SEM. All comparisons were carried out with one-way ANOVA and Student's t test. **p < 0.01; *p < 0.05; NS, not significant (p > 0.05). Scale bars, 10 μm.
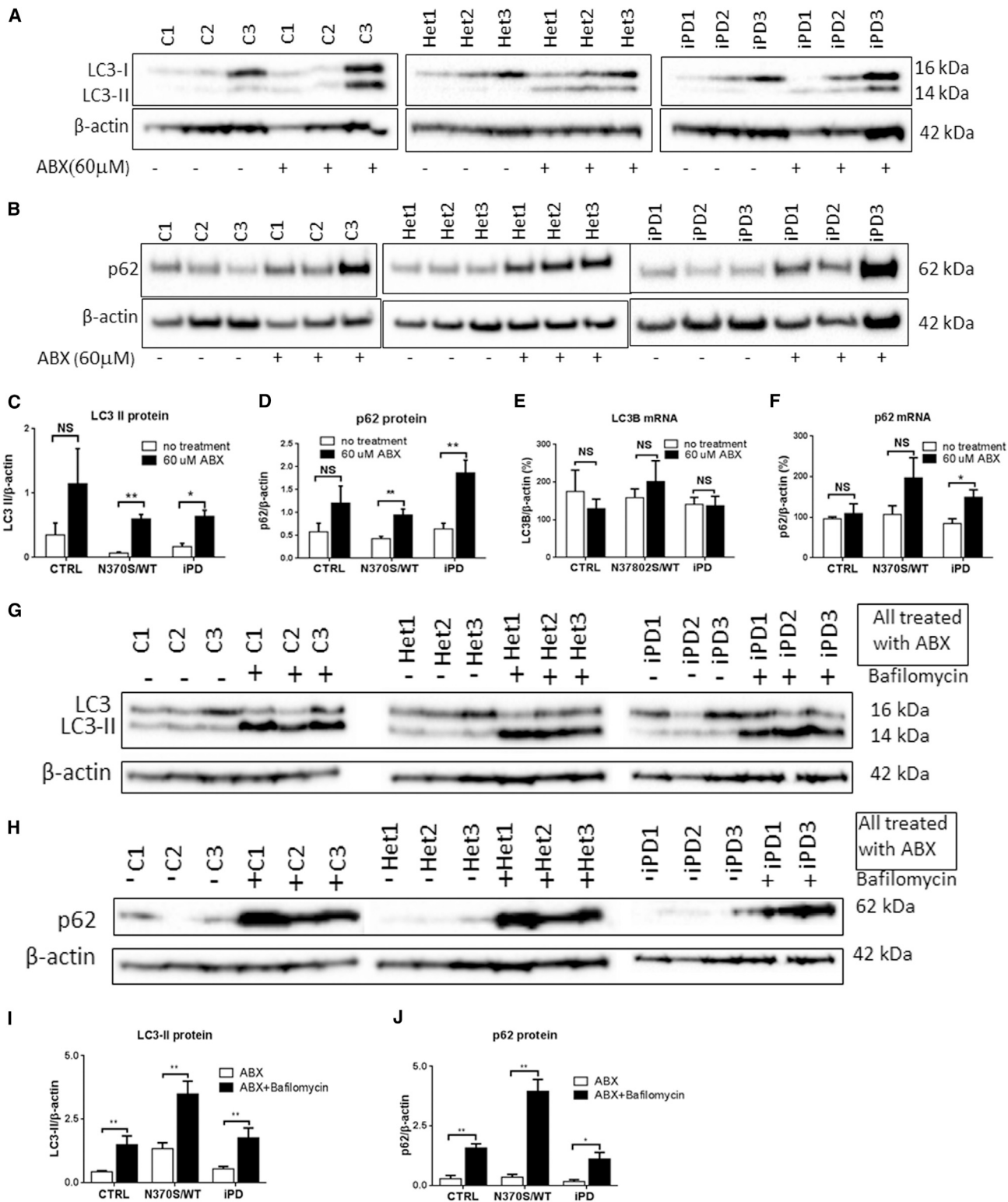
Figure 7. Ambroxol Treatment Upregulates Macroautophagy and Rescues the Autophagic Defect

(A–D) Following ambroxol (ABX) treatment, levels of the autophagosome markers LC3-II and p62 were significantly increased in *GBA1* mutation (Het1–3; N370S/wt) and iPD (iPD1–3) cell lines, but not in control (C1–3; CTRL) cells.

(legend continued on next page)

cover the tissue in order to prevent tissue floating in the medium. Media were changed every 4 days until migrated cells reached 60%–70% confluency. The cells were dissociated from the well with Accutase (Millipore) and seeded in normal culture dishes with growth medium. Cells were passaged with a ratio of 1:3 when they reached 70%–80% confluency. At this density, the growth medium was removed; cells were washed with PBS without Ca^{2+} and were incubated with Accutase (1 mL/dish; 100 × 20 mm) at 37°C for 3–5 min. Growth medium was added to the dissociated cells and the medium containing cells was divided over three individual dishes. Cells were cultured and maintained in growth medium at 37°C with 5% CO_2/95% air.

Neurosphere Formation and Maintenance

When haNCSC reached to 70%–80% confluency, cells were dissociated with Accutase at 37°C for 3–5 min. Growth medium was added to the dish to inhibit Accutase activity. Cells were collected and pelleted by centrifugation at 200 × g for 10 min. The cell pellet was resuspended with neurosphere formation medium, transferred to an uncoated 12-well plate, and incubated at 37°C with 5% CO_2/95% air. Neurospheres formed within 24 hr in neurosphere formation medium. The neurospheres were cultured and maintained in the same conditions with medium changes every 5 days.

Dopaminergic Neuronal Differentiation of haNCSCs with Co-culture System

PA6 cells were maintained as described previously (Kawasaki et al., 2000). For differentiation experiments, PA6 cells were seeded on fibronectin-coated chamber slides 1 day before introducing haNCSCs into the culture. haNCSCs were harvested and resuspended in neurobasal medium supplemented with B27 (1×). The medium was removed from the chamber and PA6 cells were washed with PBS once. haNCSC cells in neurobasal medium supplemented with B27 were introduced into the chamber with a density of 200 cells/chamber. Medium was changed every 2 days up to 40 days.

Dopaminergic Neuronal Differentiation with Defined Medium and Quantification

haNCSC were detached with Accutase solution and the Accutase was neutralized by the addition of growth medium. Cells were seeded in fibronectin-coated 6-well plates at a density of 2.4 × 10^4 cells/well (for immunocytochemistry assay, cells were seeded onto coverslips coated with fibronectin within a 6-well plate) with growth medium. After 24 hr of seeding, the growth medium was removed from the well; cells were washed once with neurobasal

medium and then cultured with neuronal induction medium. The cells were cultured with 5% CO_2/95% air for 10 days for neuronal induction. Following neuronal induction, the neuronal induction medium was replaced with neuronal maturation medium. The cells were cultured with 5% CO_2/95% air for 30 days. The volume of neuronal maturation medium was 1.7–2 mL/well (6-well plate). The medium was changed with the freshly made neuronal maturation medium every 8 days during maturation. For the purposes of assessing the percentage of dopaminergic neurons in the differentiated cells, the number of total cells and TH-positive immunostaining neurons were counted. For the three groups each group contained three subjects, three slides of each subject were studied, and three fields of each slide were used for counting. The percentage of dopaminergic neurons was then calculated according to the counts.

Ambroxol Treatment of haNCSC-Derived Neurons

haNCSC-derived neuronal cultures were treated at day 40 of neuronal differentiation with ambroxol (A9797, Sigma-Aldrich) on alternate days for 6 days. Ambroxol was dissolved in DMSO and further diluted in cell culture medium to give a final concentration of 60 μM. Controls were cultured with medium containing DMSO instead of ambroxol in DMSO. At day 6, the cells were washed twice with PBS prior to harvest. Cell pellets were frozen at −80°C for storage.

Statistical Analysis

Data are expressed as mean ± SEM and statistical significance between groups was determined by one-way ANOVA followed by the two-tailed t test. A p value of <0.05 was considered significantly different. All data were analyzed by GraphPad Prism 6 statistical software.

(E) LC3B mRNA levels were not significantly different between treated and untreated groups.

(F) p62 mRNA levels were increased in iPD neurons after ambroxol treatment, but the increase was not statistically significant in control and *GBA1* mutation cells.

(G–J) When the macroautophagy pathway was inhibited with bafilomycin in the ambroxol-treated neurons, LC3-II and p62 levels were increased further, indicating that the fusion of lysosomes with autophagosomes is normal but the autophagosome number is increased by the ambroxol treatment in *GBA1* mutation and iPD groups.

For all three groups n = 3 cell lines; data are presented as means ± SEM. All comparisons were carried out with one-way ANOVA and Student's t test. **p < 0.01; *p < 0.05; NS, not significant (p > 0.05).

designed research studies, analyzed data, obtained funding, and wrote the manuscript.

REFERENCES

Alcalay, R.N., Dinur, T., Quinn, T., Sakanaka, K., Levy, O., Waters, C., Fahn, S., Dorovski, T., Chung, W.K., Pauciulo, M., et al. (2014). Comparison of Parkinson risk in Ashkenazi Jewish patients with Gaucher disease and GBA heterozygotes. JAMA Neurol. 71, 752–757.

Ambrosi, G., Ghezzi, C., Zangaglia, R., Levandis, G., Pacchetti, C., and Blandini, F. (2015). Ambroxol-induced rescue of defective glucocerebrosidase is associated with increased LIMP-2 and saposin C levels in GBA1 mutant Parkinson's disease cells. Neurobiol. Dis. 82, 235–242.

Awad, O., Sarkar, C., Panicker, L.M., Miller, D., Zeng, X., Sgambato, J.A., Lipinski, M.M., and Feldman, R.A. (2015). Altered TFEB-mediated lysosomal biogenesis in Gaucher disease iPSCs-derived neuronal cells. Hum. Mol. Genet. 24, 5775–5788.

Beavan, M.S., and Schapira, A.H. (2013). Glucocerebrosidase mutations and the pathogenesis of Parkinson disease. Ann. Med. 45, 511–521.

Bjorkoy, G., Lamark, T., Brech, A., Outzen, H., Perander, M., Overvatn, A., Stenmark, H., and Johansen, T. (2005). p62/SQSTM1 forms protein aggregates degraded by autophagy and has a protective effect on huntingtin-induced cell death. J.Cell Biol. 171, 603–614.

Brito, J.M., Teillet, M.A., and Le Douarin, N.M. (2006). An early role for sonic hedgehog from foregut endoderm in jaw development: ensuring neural crest cell survival. Proc. Natl. Acad. Sci. USA 103, 11607–11612.

Buitrago-Delgado, E., Nordin, K., Rao, A., Geary, L., and LaBonne, C. (2015). Shared regulatory programs suggest retention of blastula-stage potential in neural crest cells. Science 348, 1332–1335.

Calloni, G.W., Glavieux-Pardanaud, C., Le Douarin, N.M., and Dupin, E. (2007). Sonic Hedgehog promotes the development of multipotent neural crest progenitors endowed with both mesenchymal and neural potentials. Proc. Natl. Acad. Sci. USA 104, 19879–19884.

Cleeter, M.W., Chau, K.Y., Gluck, C., Mehta, A., Hughes, D.A., Duchen, M., Wood, N.W., Hardy, J., Mark, C.J., and Schapira, A.H. (2013). Glucocerebrosidase inhibition causes mitochondrial dysfunction and free radical damage. Neurochem. Int. 62, 1–7.

de Lau, L.M., and Breteler, M.M. (2006). Epidemiology of Parkinson's disease. Lancet Neurol. 5, 525–535.

Ebrahimi-Fakhari, D., McLean, P.J., and Unni, V.K. (2012). Alpha-synuclein's degradation in vivo: opening a new (cranial) window on the roles of degradation pathways in Parkinson disease. Autophagy 8, 281–283.

Gegg, M.E., Burke, D., Heales, S.J., Cooper, J.M., Hardy, J., Wood, N.W., and Schapira, A.H. (2012). Glucocerebrosidase deficiency in substantia nigra of Parkinson disease brains. Ann. Neurol. 72, 455–463.

Hauser, S., Widera, D., Qunneis, F., Muller, J., Zander, C., Greiner, J., Strauss, C., Luningschror, P., Heimann, P., Schwarze, H., et al. (2012). Isolation of novel multipotent neural crest-derived stem cells from adult human inferior turbinate. Stem Cells Dev. 21, 742–756.

Itakura, E., and Mizushima, N. (2011). p62 Targeting to the autophagosome formation site requires self-oligomerization but not LC3 binding. J.Cell Biol. 192, 17–27.

Kawasaki, H., Mizuseki, K., Nishikawa, S., Kaneko, S., Kuwana, Y., Nakanishi, S., Nishikawa, S.I., and Sasai, Y. (2000). Induction of midbrain dopaminergic neurons from ES cells by stromal cell-derived inducing activity. Neuron 28, 31–40.

Kim, J., Lo, L., Dormand, E., and Anderson, D.J. (2003). SOX10 maintains multipotency and inhibits neuronal differentiation of neural crest stem cells. Neuron 38, 17–31.

Le Douarin, N.M., Creuzet, S., Couly, G., and Dupin, E. (2004). Neural crest cell plasticity and its limits. Development 131, 4637–4650.

Levy, O.A., Malagelada, C., and Greene, L.A. (2009). Cell death pathways in Parkinson's disease: proximal triggers, distal effectors, and final steps. Apoptosis 14, 478–500.

Litvan, I., Bhatia, K.P., Burn, D.J., Goetz, C.G., Lang, A.E., McKeith, I., Quinn, N., Sethi, K.D., Shults, C., and Wenning, G.K. (2003). Movement disorders society scientific issues committee report: SIC task force appraisal of clinical diagnostic criteria for parkinsonian disorders. Mov. Disord. 18, 467–486.

Manning-Bog, A.B., Schule, B., and Langston, J.W. (2009). Alpha-synuclein-glucocerebrosidase interactions in pharmacological Gaucher models: a biological link between Gaucher disease and parkinsonism. Neurotoxicology 30, 1127–1132.

Mazzulli, J.R., Xu, Y.H., Sun, Y., Knight, A.L., McLean, P.J., Caldwell, G.A., Sidransky, E., Grabowski, G.A., and Krainc, D. (2011). Gaucher disease glucocerebrosidase and alpha-synuclein form a bidirectional pathogenic loop in synucleinopathies. Cell 146, 37–52.

Mazzulli, J.R., Zunke, F., Tsunemi, T., Toker, N.J., Jeon, S., Burbulla, L.F., Patnaik, S., Sidransky, E., Marugan, J.J., Sue, C.M., and Krainc, D. (2016). Activation of beta-glucocerebrosidase reduces pathological alpha-synuclein and restores lysosomal function in Parkinson's patient midbrain neurons. J. Neurosci. 36, 7693–7706.

McNeill, A., Magalhaes, J., Shen, C., Chau, K.Y., Hughes, D., Mehta, A., Foltynie, T., Cooper, J.M., Abramov, A.Y., Gegg, M., and Schapira, A.H. (2014). Ambroxol improves lysosomal biochemistry in glucocerebrosidase mutation-linked Parkinson disease cells. Brain 137, 1481–1495.

Mizushima, N., Levine, B., Cuervo, A.M., and Klionsky, D.J. (2008). Autophagy fights disease through cellular self-digestion. Nature *451*, 1069–1075.

Murphy, K.E., Gysbers, A.M., Abbott, S.K., Tayebi, N., Kim, W.S., Sidransky, E., Cooper, A., Garner, B., and Halliday, G.M. (2014). Reduced glucocerebrosidase is associated with increased alpha-synuclein in sporadic Parkinson's disease. Brain *137*, 834–848.

Nagoshi, N., Shibata, S., Kubota, Y., Nakamura, M., Nagai, Y., Satoh, E., Morikawa, S., Okada, Y., Mabuchi, Y., Katoh, H., et al. (2008). Ontogeny and multipotency of neural crest-derived stem cells in mouse bone marrow, dorsal root ganglia, and whisker pad. Cell Stem Cell *2*, 392–403.

Okita, K., Matsumura, Y., Sato, Y., Okada, A., Morizane, A., Okamoto, S., Hong, H., Nakagawa, M., Tanabe, K., Tezuka, K., et al. (2011). A more efficient method to generate integration-free human iPS cells. Nat. Methods *8*, 409–412.

Sardi, S.P., Cheng, S.H., and Shihabuddin, L.S. (2015). Gaucher-related synucleinopathies: the examination of sporadic neurodegeneration from a rare (disease) angle. Prog. Neurobiol. *125*, 47–62.

Schapira, A.H. (2015). Glucocerebrosidase and Parkinson disease: recent advances. Mol. Cell Neurosci. *66*, 37–42.

Schapira, A.H., and Gegg, M.E. (2013). Glucocerebrosidase in the pathogenesis and treatment of Parkinson disease. Proc. Natl. Acad. Sci. USA *110*, 3214–3215.

Schapira, A.H., and Jenner, P. (2011). Etiology and pathogenesis of Parkinson's disease. Mov. Disord. *26*, 1049–1055.

Schapira, A.H., Olanow, C.W., Greenamyre, J.T., and Bezard, E. (2014). Slowing of neurodegeneration in Parkinson's disease and Huntington's disease: future therapeutic perspectives. Lancet *384*, 545–555.

Schondorf, D.C., Aureli, M., McAllister, F.E., Hindley, C.J., Mayer, F., Schmid, B., Sardi, S.P., Valsecchi, M., Hoffmann, S., Schwarz, L.K., et al. (2014). iPSC-derived neurons from GBA1-associated Parkinson's disease patients show autophagic defects and impaired calcium homeostasis. Nat. Commun. *5*, 4028.

Sevlever, D., Jiang, P., and Yen, S.H. (2008). Cathepsin D is the main lysosomal enzyme involved in the degradation of alpha-synuclein and generation of its carboxy-terminally truncated species. Biochemistry *47*, 9678–9687.

Shan, T., Liu, W., and Kuang, S. (2013). Fatty acid binding protein 4 expression marks a population of adipocyte progenitors in white and brown adipose tissues. FASEB J. *27*, 277–287.

Sidransky, E., Nalls, M.A., Aasly, J.O., Aharon-Peretz, J., Annesi, G., Barbosa, E.R., Bar-Shira, A., Berg, D., Bras, J., Brice, A., et al. (2009). Multicenter analysis of glucocerebrosidase mutations in Parkinson's disease. N. Engl. J. Med. *361*, 1651–1661.

Siebert, M., Sidransky, E., and Westbroek, W. (2014). Glucocerebrosidase is shaking up the synucleinopathies. Brain *137*, 1304–1322.

Stemple, D.L., and Anderson, D.J. (1992). Isolation of a stem cell for neurons and glia from the mammalian neural crest. Cell *71*, 973–985.

Thomas, S., Thomas, M., Wincker, P., Babarit, C., Xu, P., Speer, M.C., Munnich, A., Lyonnet, S., Vekemans, M., and Etchevers, H.C. (2008). Human neural crest cells display molecular and phenotypic hallmarks of stem cells. Hum. Mol. Genet. *17*, 3411–3425.

Tiwari, N., Meyer-Schaller, N., Arnold, P., Antoniadis, H., Pachkov, M., van, N.E., and Christofori, G. (2013). Klf4 is a transcriptional regulator of genes critical for EMT, including Jnk1 (Mapk8). PLoS One. *8*, e57329.

Trzaska, K.A., and Rameshwar, P. (2011). Dopaminergic neuronal differentiation protocol for human mesenchymal stem cells. Methods Mol. Biol. *698*, 295–303.

Volta, M., Milnerwood, A.J., and Farrer, M.J. (2015). Insights from late-onset familial parkinsonism on the pathogenesis of idiopathic Parkinson's disease. Lancet Neurol. *14*, 1054–1064.

Wada, N., Javidan, Y., Nelson, S., Carney, T.J., Kelsh, R.N., and Schilling, T.F. (2005). Hedgehog signaling is required for cranial neural crest morphogenesis and chondrogenesis at the midline in the zebrafish skull. Development *132*, 3977–3988.

Xilouri, M., Vogiatzi, T., Vekrellis, K., and Stefanis, L. (2008). alpha-synuclein degradation by autophagic pathways: a potential key to Parkinson's disease pathogenesis. Autophagy *4*, 917–919.

Supplemental Information

A Human Neural Crest Stem Cell-Derived Dopaminergic Neuronal Model Recapitulates Biochemical Abnormalities in *GBA1* Mutation Carriers

Shi-Yu Yang, Michelle Beavan, Kai-Yin Chau, Jan-Willem Taanman, and Anthony H.V. Schapira
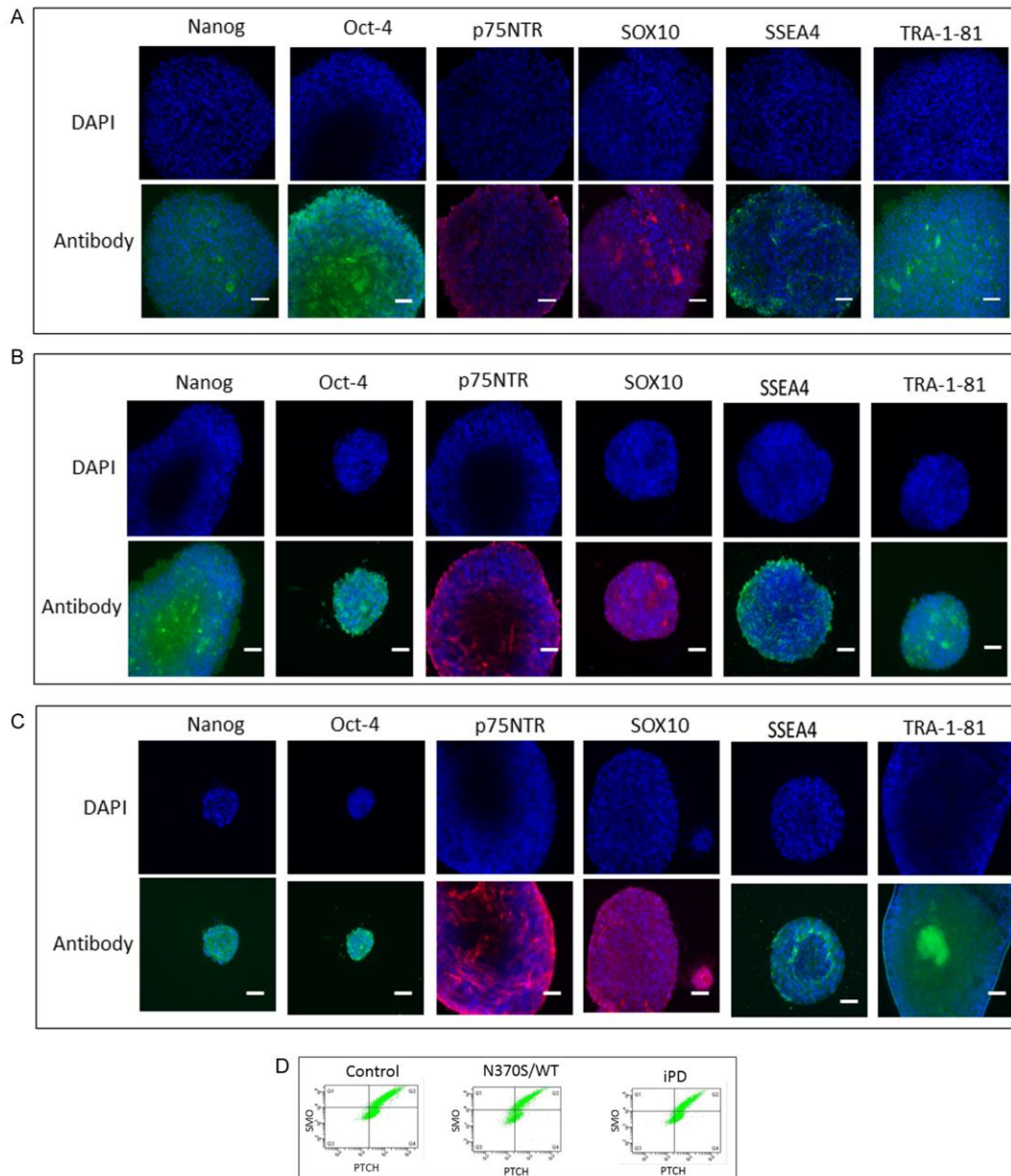
Figure S1 (related to Fig 1) Comparison of pluripotent properties between adipose neural crest stem cells derived from control, GBA mutant and iPD subjects.

To examine whether there are differences in the pluripotent properties of adipose neural crest stem cells derived from control, carriers of a *GBA1* mutation and iPD patients, the expression of pluripotency genes (*NANOG, OCT4, SSEA4, TRA-1-81*, all green) and the neural crest genes (*p75NTR* and *SOX10*, all red) were examined with immunochemistry. All cells derived from control (A), heterozygous mutant *GBA1* (B) and iPD (C) subjects express pluripotency and neural crest genes. There was no noticeable difference in the expression of these genes between control, heterozygous mutant *GBA1* and iPD subjects. The expression of sonic hedgehog (a signalling molecule involved in the development of early neural crest progenitors) was examined by FACS analysis. There was no obvious difference in the expression of sonic hedgehog between control, heterozygous mutant *GBA1* and iPD subjects (D). Nuclei were stained with DAPI (blue). (Bars: 50 mm)
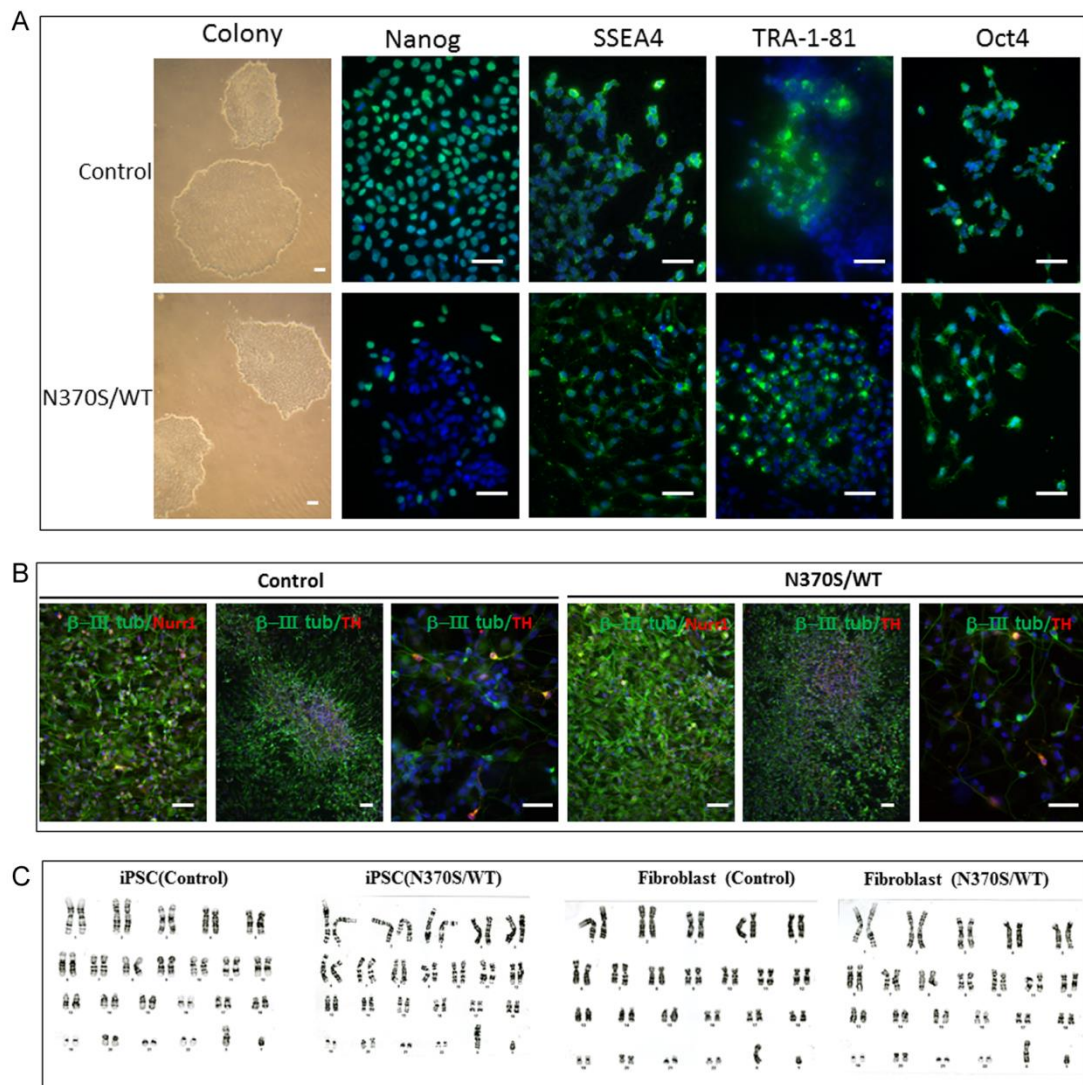
Figure S2 (related to Fig 3)
The iPSC clones from both control and mutant subjects expressed pluripotency genes (*NANOG, SSEA4, TRA-1-81* and *OCT4*, all green) (A). The iPSC stem cells were differentiated into dopaminergic neurons which expressed the neuronal marker, b-III tubulin (b-III tubulin, green) and the dopaminergic neuronal markers tyrosine hydroxylase (TH, red) and nuclear receptor related protein 1 (NURR1, red) (B). Karyotyping (C) was performed to examine the integrity of the chromosomes in fibroblast and iPSC derived from control subjects and subjects with the *GBA1* mutation. Nuclei were stained with DAPI (Blue). (Bars: 50 mm)
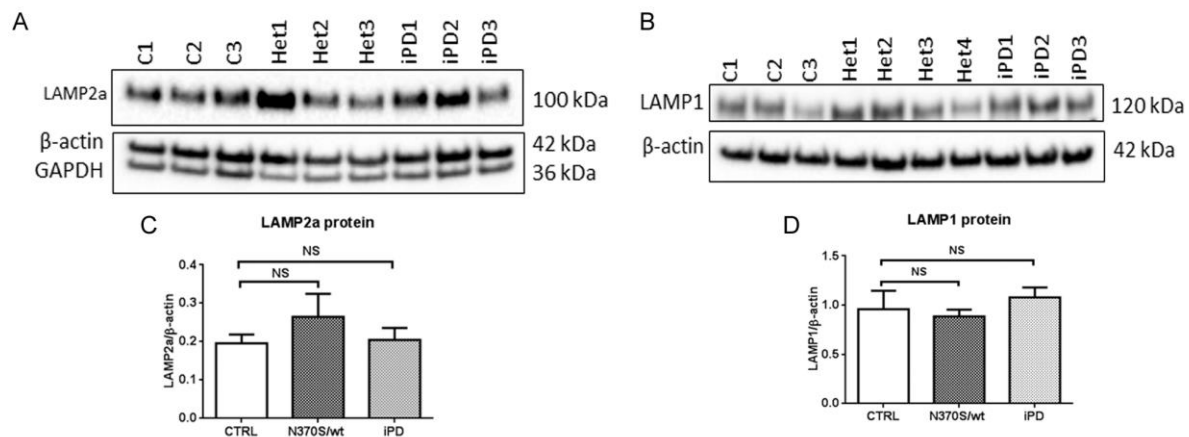
Figure S3 (related to Fig 5)

The levels of lysosomal proteins such as LAMP2a (A and C) and LAMP1 (B and D) were not significantly different between the 3 groups. This suggests that the lysosomal content is not affected by the *GBA 1* mutation in human neuronal cells. For all groups n=3-4 cell lines, error bars reflect SEM. All comparisons were carried out with one-way ANOVA and Student's t-test NS: p>0.05.

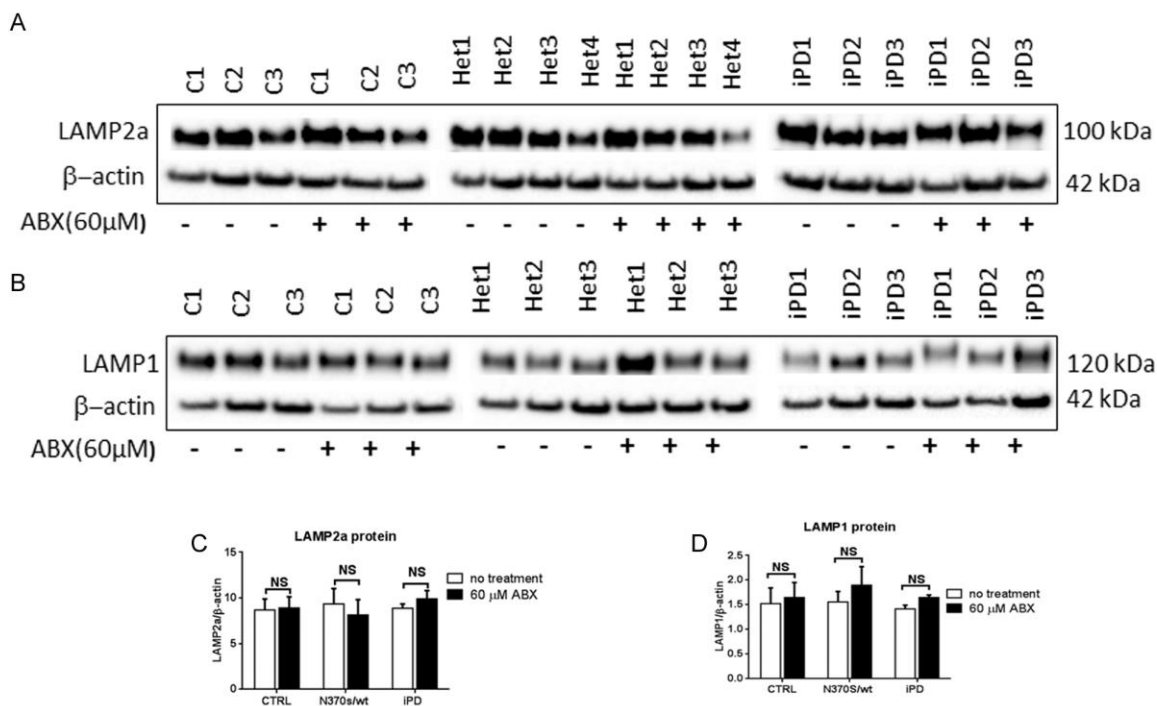Figure S4 (related to Fig 5)
The level of the lysosomal proteins LAMP2a (A and C) and LAMP1 (B and D) was not affected by ambroxol treatment in the three groups, suggesting that ambroxol treatment is not causing an overall expansion of lysosomal compartment. For all groups n=3-4 (cell lines), error bars reflect SEM. All comparisons were carried out with one-way ANOVA and Student's t-test   NS: p>0.05.

Table S1 **Summary of patient-derived adipose neural crest stem cells**

Subject	Genotype	Gender	Diagnosis	Age at biopsy
C1	wt/wt	Female	CTRL	67
C2	wt/wt	Female	CTRL	70
C3	wt/wt	Male	CTRL	81
Het1	N370S/wt	Female	*GBA* Carrier	82
Het2	N370S/wt	Male	*GBA* Carrier	52
Het3	N370S/wt	Female	*GBA* Carrier	67
Het4	N370S/wt	Male	GBA-PD	80
PD1	wt/wt	Male	iPD	80
PD2	wt/wt	Female	iPD	75
PD3	wt/wt	Female	iPD	53

Table S2 **List of antibodies**

Antibody	Dilution	Application	Source	Cat. No.
P75NGF R	1:500	ICC	Abcam	ab8874
SOX 10	1:250	ICC	Santa Cruz	sc17342
Nestin	1:500	ICC	Millipore	mab5326
Fatty Acid-binding protein 4	1:100	ICC	R &D system	af3150
SSEA-4	1:100	ICC	Abcam	Ab16287
Nanog	1:500	ICC	Abcam	Ab17336
OCT-4	1:250	ICC	Millipore	MAB4401
LMX1	1:250	ICC	Millipore	MAB10533
PTCH	1:500	FACS	Abcam	Ab129341
SMO	1:50	FACS	Millipore	MAB360
Beta III Tubulin	1:500	WB/ICC	Abcam	ab18207
Tyrosine Hydroxylase	1:1000	WB/ICC	Abcam	ab6211
Nurr1	1:200	ICC	Abcam	ab55769
Dopamine transporter	1:1000	ICC	Millipore	Ab5802
GBA	1:1500	WB	Calbiochem	AP1140
β-ACTIN	1:5000	WB	Abcam	ab8227
BiP	1:1000	WB	Abcam	ab21685
LAMP1	1:1000	WB	Abcam	Ab24170
LAMP2a	1:500	WB	Abcam	ab18528
Hsc70	1:1000	WB	Abcam	ab51052
GAPDH	1:5000	WB	Abcam	ab9485
LC3	1:1000	WB	Cell Signaling	2775
p62	1:1500	WB	BD Biosciences	610832
Alpha-synuclein	1:500	WB/ICC	Abcam	ab1903

Table S3 **List of PCR primers**

Pluripotent genes	Forward/reverse primers	Sequences of Primers
SOX2	Forward	GCTACAGCATGATGCAGGACCA
	Reverse	TCTGCGAGCTGGTCATGGAGTT
Oct4	Forward	CCTGAAGCAGAAGAGGATCACC
	Reverse	AAAGCGGCAGATGGTCGTTTGG
Nanog	Forward	CTCCAACATCCTGAACCTCAGC
	Reverse	CGTCACACCATTGCTATTCTTCG
Rex1	Forward	GGAAATAGCAGAGTGCTTCGC
	Reverse	CTCTTCTGTTCTGTTCACACAG
cMYC	Forward	CTGAGACAGATCAGCAACAACC
	Reverse	TCTTTTATGCCCAAAGTCCAAT
KLF4	Forward	CATCTCAAGGCACACCTGCGAA
	Reverse	TCGGTCGCATTTTTGGCACTGG

Supplemental Experimental Procedures

GBA1 **Screening**: *GBA1* mutation status in all participants was confirmed by sequencing exons 1 to 11 of the *GBA1* gene, using a published protocol (Neumann et al. 2009)with polymerase chain reaction (PCR) primers designed exclusively for regions of the *GBA1* gene not found in the pseudogene. After amplification by PCR the product was run on a 1% agarose gel with ethidium bromide and size-checked to ensure it was not the pseudogene. Sanger sequencing was performed for each exon and flanking intronic sequences using the Dye Terminator Sequencing Kit (Applied Bio-systems) on an ABI 3700xl genetic analyser.

Growth medium: DMEM, (High Glucose, Gutamax, Life technologies) supplemented with foetal bovine serum (10%), Sodium Pyruvate (1 mM), Uridine (50 µg/ml), Penicillin (50 units/ml), Streptomycin (50 µg/ml), Fungizone (Amphotericin B, 1.25 µg/ml).

Neurosphere formation medium: DMED/F12 (1:1, Glutamax, Life technologies) supplemented with B27 supplement (1x, Life technologies), recombinant human FGF basic (146 aa) (20 ng/ml, R&D Systems), recombinant human EGF (10 ng/ml, AbD Serotec), recombinant human leukemia inhibitory factor (10 ng/ml, Sigma), Penicillin (50 units/ml), Streptomycin (50 µg/ml),Fungizone (1.25 µg/ml).

Neuronal induction medium (first 10 days of differentiation): Neurobasal medium supplemented with B-27 supplement (1x), recombinant Human Sonic Hedgehog (250 ng/ml, R&D Systems), recombinant Human/Mouse FGF-8b (100 ng/ml), Recombinant Human FGF basic (50 ng/ml), Penicillin (50 units/ml), Streptomycin (50 µg/ml),Fungizone (1.25 µg/ml).

Neuronal maturation medium: (11-40 days of differentiation): Neuronal induction medium further supplemented with recombinant Human/Mouse/Rat/Canine/Equine BDNF (50 ng/ml, R&D Systems).

Flow cytometry: Cells were detached with accutase solution, washed with PBS containing 1% foetal bovine serum and pelleted by centrifuging for 10 minutes at 200 × *g*. Cells were fixed with 2% paraformaldehyde for 30 minutes on ice and incubated with anti-smoothened (SMO) and anti-patched (PTCH) antibodies on ice for 30 minutes. Following washing secondary antibodies were incubated on ice for 30 minutes. Cells were immediately analysed by BD FACScan. BD CellQuest software (BD Biosciences) was used for analyses. Primary antibody isotype control and unlabelled cells (no primary and secondary antibodies) were used for FACS gating.

iPSCs generation and dopaminergic neuronal differentiation: Yamanaka plasmids were purchased from Addgene. Plasmids including pCXLE h*Oct4 shp53-F*, *pCXLE hSK* and *pCXLE hUL* have been previously described (Okita et al. 2011). Early passage fibroblasts (less than 12 passages) in logarithmic growth phase were used for iPSC generation. Fibroblasts were harvested; the cell pellet was washed once with PBS and suspended in resuspension buffer (Neon Transfection System, Invitrogen). 10^6 cells were transfected with 1 µg DNA of each plasmid using the Neon transfection system (Invitrogen). 2×10^5 viable cells were transferred into one well of a 6 well plate coated with hES cell qualified Matrigel with growth medium. After 24 hours of transfection, growth medium was replaced with mTESR1 (StemCellTechnologies) medium supplemented with sodium butyrate (0.5 mM). Following 12 days of transfection, mTESR1 medium alone was used. Medium was changed daily for the whole period of iPSC generation. After 30 days of transfection, the whole well was stained with TRA-1-81 antibody and positive colonies were selected and isolated for further characterisation and differentiation.

iPSCs were differentiated into dopaminergic neurons with a midbrain dopaminergic neuronal induction method (Kriks et al. 2011; Stanslowsky et al. 2014).

Karyotyping: Karyotyping was performed by full G-band analysis of 20 cells in 3 human iPSC cultures (1x wild type, 1x heterozygous *GBA1* mutation carrier, and 1x iPD) to examine the integrity of the chromosomes by The Doctor's Laboratory at Whitfield Street, London. All cells tested showed a normal banding pattern.

Immunochemistry: Cells were washed with PBS two times, each wash lasting 5 minutes. Cells were fixed with 4% paraformaldehyde for 15 minutes at room temperature and subsequently permeabilized with 0.25% Triton X-100 for 15 minutes. Following three washings, cells were blocked with 10% goat serum in PBS for 30 minutes and incubated with primary antibodies overnight at 4°C. Appropriate secondary antibodies conjugated with fluorescein were used to visualize the primary antibodies. Details of primary and secondary antibodies and their dilution can be found in supplementary table 2.

Lysosomal enzymatic activity assays: Cell pellets were re-suspended in water and sonicated in a water-bath sonicator for 1 minute. GCase activity was determined in cell lysates of about 1 µg protein with a previous reported method (Cleeter et al. 2013).

Western blotting: Cells were harvested, washed with PBS, and processed as previously described (McNeill et al. 2014) . Proteins were extracted using urea/SDS buffer (8 M urea, 2% SDS, 10 mM Tris·HCl pH 6.8) containing protease inhibitors. To limit the effect of DNA content in the protein solution, the extraction was incubated with DNase at 37°C for 1 hour to remove DNA. In total, 40 µg of protein was loaded on a 4 – 12% Bis-Tris Gel (NuPAGE, Invitrogen) and transferred to a polyvinylidene difluoride membrane (Millipore). The membrane was incubated with primary antibodies in 5% milk, PBS, 0.4%Tween 20 at room temperature for 2 hours. Following 3 washing, the membranes were incubated with the appropriate secondary antibodies conjugated to horseradish peroxidase for 1 hour at room temperature. The bands were visualized with Clarity ECL Western Blotting Substrate (Bio-Rad). Analyses were carried out

using Image Lab software (BioRad). The details of primary and secondary antibodies and their dilution can be found in supplemental table 2. .

Autophagy studies: Where indicated, cells were treated with 0.2 µM bafilomycin (EMD, Millipore) for 4 hours at 37 °C in the presence of 5% CO_2, and then fixed or lysed for western blot analysis. LC3/LC3-II and p62 levels were quantified using Image Lab software and normalized for β-actin. The LC3 flux was quantified by dividing levels of LC3-II after bafilomycin treatment for 6 h by the level of LC3-II without treatment.

Real time reverse transcriptase quantitative PCR (RT-qPCR): Total RNA was extracted from cell pellets with the RNeasy mMni Kit with on-column DNase digestion according to the manufacture's guidelines (Qiagen). RNA yield and quality were assessed by Nanodop UV spectrophotometry. cDNA was generated from 1.0 µg of RNA with the Quantitect Reverse Transcription Kit from Qiagen. All RT-qPCR reactions (except for p62 and LC3B) were performed using the power SYBR Green PCR master mix (Life Technologies) and assayed with the Step One Real Time PCR system (Applied Bio-system). For p62 and LC3B, qPCR reaction was performed using TaqMan Gene Expression Assays (Life Technologies; Hs01061917_g1 for human sequesosome 1 p62, Hs00797944s1 for human microtubule-associated protein 1 light chain 3 beta, Hs99999903m1 for human beta-actin) in the StepOne Real-Time PCR Systems (Life Technologies). Fold-change in gene expression was calculated using the $2^{-\Delta\Delta CT}$ method, based on biological reference samples and beta-actin messenger RNA levels for normalization. All the results were obtained from the evaluation of two technical duplicates of three independent experiments.

Supplemental References

Cleeter, M.W., Chau, K.Y., Gluck, C., Mehta, A., Hughes, D.A., Duchen, M., Wood, N.W., Hardy, J., Mark, C.J., & Schapira, A.H. 2013. Glucocerebrosidase inhibition causes mitochondrial dysfunction and free radical damage. *Neurochem.Int.*, 62, (1) 1-7

Kriks, S., Shim, J.W., Piao, J., Ganat, Y.M., Wakeman, D.R., Xie, Z., Carrillo-Reid, L., Auyeung, G., Antonacci, C., Buch, A., Yang, L., Beal, M.F., Surmeier, D.J., Kordower, J.H., Tabar, V., & Studer, L. 2011. Dopamine neurons derived from human ES cells efficiently engraft in animal models of Parkinson's disease. *Nature*, 480, (7378) 547-551

McNeill, A., Magalhaes, J., Shen, C., Chau, K.Y., Hughes, D., Mehta, A., Foltynie, T., Cooper, J.M., Abramov, A.Y., Gegg, M., & Schapira, A.H. 2014. Ambroxol improves lysosomal biochemistry in glucocerebrosidase mutation-linked Parkinson disease cells. *Brain*, 137, (Pt 5) 1481-1495

Neumann, J., Bras, J., Deas, E., O'Sullivan, S.S., Parkkinen, L., Lachmann, R.H., Li, A., Holton, J., Guerreiro, R., Paudel, R., Segarane, B., Singleton, A., Lees, A., Hardy, J., Houlden, H., Revesz, T., & Wood, N.W. 2009. Glucocerebrosidase mutations in clinical and pathologically proven Parkinson's disease. *Brain*, 132, (Pt 7) 1783-1794

Okita, K., Matsumura, Y., Sato, Y., Okada, A., Morizane, A., Okamoto, S., Hong, H., Nakagawa, M., Tanabe, K., Tezuka, K., Shibata, T., Kunisada, T., Takahashi, M., Takahashi, J., Saji, H., & Yamanaka, S. 2011. A more efficient method to generate integration-free human iPS cells. *Nat.Methods*, 8, (5) 409-412

Stanslowsky, N., Haase, A., Martin, U., Naujock, M., Leffler, A., Dengler, R., & Wegner, F. 2014. Functional differentiation of midbrain neurons from human cord blood-derived induced pluripotent stem cells. *Stem Cell Res.Ther.*, 5, (2) 35